Journal of the European Ceramic Society **18** (1998) 429–444

PII: S0955-2219(97)00146-5
0955-2219/98/$19.00 + 0.00

Characterization of Dielectric Powders by a New Defined Form Factor

Heinz Ragossnig and Adalbert Feltz

Siemens Matsushita Components OHG, Deutschlandsberg Siemensstraβe 43, A-8530, Deutschlandsberg, Austria

(Received 17 March 1997; accepted 3 July 1997)

Abstract

Capacitance measurements of oxide powders in the frequency range of 1 kHz to 10 MHz have been performed in order to deduce a form factor which is related to the morphology of the particles and their arrangement in the powder. Using a capacitor measuring setup the frequency independent real part of the complex dielectric constant was measured in the range of 1 kHz to 2 MHz in dependence on the volume fraction. The interpretation follows the models derived for inhomogeneous dielectrics, which allow to calculate a morphology dependent parameter provided that the permittivity of the solid is known. A new defined form dependent weighting factor introduced in Bruggeman's model of geometrical averaging between lamellar and spherical constituents is shown to supply the better approximation to measuring data than the aspect ratio of ellipsoids determining the depolarization factor. The results are verified for aggregated and partially stepwise ground powders of Mg_2TiO_4, $MgAl_2O_4$, $SrTiO_3$, $CaTiO_3$, Al_2O_3, and ZnO and related to other particle shape parameters derived from SEM studies indicating very clearly the suitability to describe the morphology of powders by this new form factor. The frequently applied Lichtenecker rule does not allow to consider particle morphology. For comparison the specific surface area BET data and the d_{50} values from grain size distribution measurements of the powders are also reported. The applicability of the method for checking the reproducibility of different lots of capacitor raw materials is shown for two COG powders. © *1998 Published by Elsevier Science Limited.*

Zusammenfassung

Es wird über Kapazitätsmessungen an Oxidpulvern im Frequenzbereich 1 kHz bis 10 MHz und deren Auswertung zwecks Ermittlung eines Formparameters berichtet, der zur Morphologie der Partikel und deren Anordnung im Pulver in Beziehung steht. Mit Hilfe einer Kondensator - Meßanordnung wird für die Pulver im Bereich bis zu 2 MHz der frequenzunabhängige Realteil der komplexen Dielektrizitätskonstante in Abhängigkeit vom Volumenbruch ermittelt. Die Auswertung folgt den für inhomogene Dielektrika abgeleiteten Modellen, die bei Kenntnis der DK des betreffenden Feststoffes einen morphologieabhängigen Formparameter zu berechnen gestatten. Die Definition eines formabhängigen Gewichtsfaktors im Rahmen der von Bruggeman vorgeschlagenen geometrischen Mittelung zwischen lamellaren und sphärischen Konfigurationsanteilen liefert eine bessere Beschreibung der Meßwerte als das Aspektverhältnis von Ellipsoiden, das in die klassische Gleichung für den Entelektrisierungsfaktor eingeht. Am Beispiel aggregierter und zum Teil in mehreren Stufen fein gemahlener Pulver von Mg_2TiO_4, $MgAl_2O_4$, $SrTiO_3$, $CaTiO_3$, Al_2O_3, und ZnO wird durch Vergleich mit anderen aus REM-Studien erhaltenen Formparametern gezeigt, daß der neu definierte Gewichtsfaktor als Formparameter zur Beschreibung der Partikelmorphologie herangezogen werden kann. In der vielfach angewandten Lichtenecker - Regel bleibt demgegenüber die Partikelmorphologie unberücksichtigt. Zum Vergleich werden jeweils die BET - Werte für die spezifische Oberfläche und der d_{50} Wert aus der Korngrößenverteilung angegeben. Die Eignung der Methode zur Kontrolle der Chargenreproduzierbarkeit von Kondensatorpulvern wird am Beispiel zweier COG-Massen aufgezeigt.

1 Introduction

The preparation of electronic ceramic devices, e.g. of thermistors, varistors, multilayer capacitors or microwave resonators requires to start from highly purified raw materials. Moreover, as a prerequisite for successful processing the knowledge of the morphological powder properties and their constancy lot by lot have to be obeyed. The latter

involves the availability of suitable examination methods. The commonly applied tests, e.g. analyses to control the chemical composition including impurities and the determination of the morphological parameters by a gas adsorption isotherm according to Brunauer, Emmett and Teller BET and grain size distribution measurements habe been frequently found to be insufficient. Therefore, there is a demand to have available some more characteristics which could be suitable to satisfy the increasing pretensions regarding reliability and smaller permissible variations of the properties of electronic ceramic devices.

It is the aim of this paper to define a form factor pertinent to the shape of the particles, which will be deduced from the dielectric properties of the powder. Different models developed for inhomogeneous dielectrics described in the literature are proved in application to single-phase dielectric powders of known composition, structure and morphology. The problem is to give an expression for the depolarization factor of a mixture of powders in air.

Especially in the low frequency range even small differences in the constitution of dielectrics give rise to differences in the frequency dependence of the permittivity. Relaxation processes prevail in this range. Variations are observed depending on the preparation conditions and frequently from lot to lot or even between samples of one and the same lot. Of course, powders of higher degree of disorder are expected to show such a behaviour in a more pronounced manner than bulk ceramics. Commonly, with increasing frequency a region of frequency independent values of the dielectric properties is achieved. However, it has to be noticed that also for bulk ceramic samples these constant permittivity data frequently are varying in the literature.

Obviously, dielectric measurements are suitable to detect small differences of the real structure of powders and even of compact ceramic samples thus indicating variations of the morphology as well as of the defect structure in the bulk of the grains and in particular at the grain boundaries and intergranular phases.

2 Powder Selection, Preparation and Characterization

The cubic spinels $MgAl_2O_4$ and Mg_2TiO_4 and the perovskites $CaTiO_3$ und $SrTiO_3$ have been selected assuming preferred formation of isometrically shaped particles in the preparation process. Such powders should be suitable for modelling of the dielectric depolarization factor. The uniaxial compounds ZnO, α-Al_2O_3 and TiO_2 (rutile) were studied for comparison. They were expected to show more pronounced an aspect ratio.

The preparation of the ternary compounds followed the mixed oxide route. Mixtures of basic magnesiumcarbonate or $CaCO_3$ or $SrCO_3$ with γ-Al_2O_3 (120 $m^2\ g^{-1}$) or highly dispersed rutile (8 $m^2\ g^{-1}$), respectively, have been heated to high temperatures as given in Table 1. Wet grinding was carried out in a first step **A** using agate spheres (10 and 20 mm $\varnothing$) in a cylinder mill. In some cases a second step **B** of fine milling followed applying a more effective excenter mill with small ZrO_2/Y_2O_3 spheres (1 mm $\varnothing$). The coarse powders formed at the high temperature during synthesis and the higher dispersed ones obtained by grinding have been measured for studying the influence of the morphological state on the dielectric properties.

Particle shape and also the fraction of primary grains have been estimated from SEM studies and partially by application of TEM.

Following Medalia,[1] from SEM and TEM photographs the shape parameters anisometry, bulkiness and roundness of the particles have been determined. The anisometry and bulkiness of a particle have been calculated from its equivalent ellipse having the same first and second degree moments about its central principal axes. For this purpose the particle was assumed to be planar and of uniform thickness and density. The anisometry was then defined as the ratio of the major axis to the minor axis of the equivalent ellipse and the bulkiness as the ratio of the ellipse area to the particle area. Moreover, the roundness defined by

$$\text{roundness} = \frac{(\text{perimeter})^2}{4\pi \cdot \text{area}}$$

has been used for particle shape characterization. The roundness is the square of the ratio of the particle perimeter to the perimeter of a circle, having the same area as the particle.

All three shape parameters are equal to 1 for spheres. The anisometry is high for elongated particles while bulkiness and roundness are high for rugged particles. The roundness parameter is also sensitive to elongation. In the case of the coarse particles with a pronounced microstructure [Fig. 1(a)] the anisometry was determined from the whole particle and the bulkiness and roundness from a particle surface photograph.

According to $S = (6/\rho d_s)$ the specific surface area values S of BET measurements may be transformed to an average value of the diameter d_s of spherical particles with density ρ. Considerable deviations are observed even in the highly dispersed

Table 1. Composition, preparation and morphological properties of the investigated powders

Compound	*Preparation conditions*	ρ_{th} g cm^{-3}	*S (BET)* m^2g^{-1}	d_S μm	*Grain size distribution*			*SEM information*			
					d_{10} μm^{-1}	d_{50} μm^{-1}	d_{90} μm^{-1}	*Appearance*	*Anisometry*	*Bulkiness*	*Roundness*
$MgAl_2O_4$											
Coarse	1200°C 10 h	3·574	9·9	0·17	1·04	4·0	13	Flake-like built aggregates and flakes $<$ 0·2 μm	1·87	1·12	4·36
Ground	Milling condition B 1·5 h		18·8	0·09	0·36	0·58	1·0	0·1 μm $<$ flakes $<$ 0·2 μm	1·83	1·12	4·90
Mg_2TiO_4											
Coarse	1300°C 10 h	3·540	0·5	3·4	38	182	288	Aggregates, coral-like structure, diameter 3 μm	1·25	1·19	10·85
Ground (a)	Milling condition A 5 h		0·6	2·8	2·9	43	126	Aggregates, coral-like structure, diameter 3 μm	1·37	1·18	9·10
Ground (b)	Milling condition A 1d		0·8	2·1	0·9	9·6	42	Aggregates, coral-like structure, diameter 3 μm	1·38	1·19	5·04
Ground (c)	Milling condition A 3d		1·4	1·2	0·58	3·2	7·9	Aggregates mainly broken down to primary particles	1·52	1·03	2·10
$CaTiO_3$											
Coarse	1150°C 4 h	4·033	1·1	1·4	1·07	7·8	29	Sponge-like porous aggregates up to 1 mm	1·28	1·16	29·63
Ground (a)	Milling condition A 5 h		1·6	0·93	0·34	1·2	6·0	Mainly broken down to small polyhedral particles	1·70	1·04	2·17
Ground (b)	Milling condition B 1·5 h		3·7	0·40	0·35	0·69	1·6	Primary polyhedral particles	1·49	1·04	1·74
$SrTiO_3$(I)											
Coarse	1000°C 10 h	5·121	2·8	0·42	0·52	2·8	11	Aggregates of about 0·3 μm primary particles	1·53	1·17	7·80
Ground	Milling condition B 1·5 h		8·2	0·14	0·20	0·31	0·50	Nonaspect shaped 0·3 μm primary particles	1·66	1·06	4·34
$SrTiO_3$(II)											
Coarse	1150°C 10 h		2·7	0·43	0·45	2·0	6·8	Aggregates of about 0·3 μm primary particles	1·53	1·17	11·24
Ground	Milling condition B 1·5 h		9·0	0·13	0·25	0·37	0·55	Nonaspect shaped 0·3 μm primary particles	1·71	1·05	3·47
ZnO	Commercial Grillo	5·675	7·9	0·13	0·3	0·5	0·8	Primary needle-like crystals prevail	2·39	1·01	1·78
α-Al_2O_3	Commercial Fluka	3·976	7·7	0·20	0·32	0·67	5·7	0·2 μm particles and aggregates up to 10 μm	1·56	1·13	4·30
TiO_2 (rutile)	Commercial Bayer	4·2503	6·2	0·23	0·25	0·38	0·57	Nonaspect shaped prim. particles	—	—	—
COGε_{60} lot 1	Commercial	5·67	3·0	0·35	0·40	0·80	2·40	Primary particles and minor aggregates	1·43	1·03	1·87
COGε_{60} lot 2	Commercial		2·9	0·36	0·30	0·57	2·90	Primary particles and minor aggregates	—	—	—
COGε_{90} lot 1	Commercial	5·40	2·6	0·43	0·40	0·80	2·80	Nonaspect shaped primary particles	—	—	—
COGε_{90} lot 2	Commercial		2·5	0·44	0·40	0·80	2·40	Nonaspect shaped primary particles	1·48	1·03	1·75

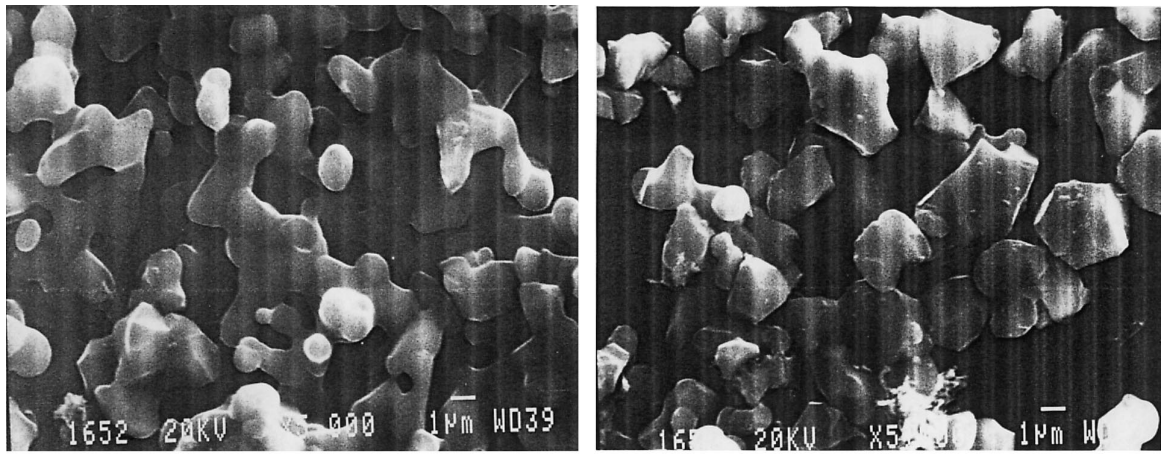

(a) (b)

Fig. 1. SEM photographs of Mg_2TiO_4 in the original coarse state formed by (a) the preparation process and (b) after grinding according to Table 1.

state of the $MgAl_2O_4$ and Mg_2TiO_4 powders comparing these data with the values d_{50} derived from laser light scattering measurements (Microtrac). Of course, the small scattering disks of more or less irregular shaped polyhedral particles measured by laser light scattering have to lead to somewhat larger d_{50} values than those obtained from calculation based on a spherical model using the specific surface area data. SEM studies [Fig. 1(a)] show that in the coarse powder state the original Mg_2TiO_4 particles are highly aggregated, which is expressed by the high bulkiness and roundness parameters listed in Table 1. In the result of grinding the part of polyhedral shaped primary particles showing partially cracks is increasing [Fig. 1(b)]. On the other hand, obviously by reason of the highly dispersed state of the components in the starting preparation mixture the $MgAl_2O_4$ original powder particles appear predominantly to consist of aggregates of more or less lamellar constituents [Fig. 2(a)]. In the ground state the particles appear planar, which leads to difficulties in obtaining a valid anisometry from the particle outline [Fig. 2(b)]. The shape parameters of the $MgAl_2O_4$ samples did not change much due to grinding.

As shown from the data of Table 1, grinding of $CaTiO_3$ and $SrTiO_3$ leads to low anisometry, bulkiness and roundness and at the same time the differences between the d_s and d_{50} values are decreasing as a result of destruction of aggregates. $SrTiO_3$ (I) and (II) have been formed by application of two different preparation conditions.

Figure 3(a) shows the TEM photograph of highly dispersed ZnO powder formed by evaporation and oxidation of Zn vapour in air (French process). Obviously, as a consequence of the hexagonal Wurtzite structure the primary particles are fine needles with a high anisometry. On the other hand, the highly dispersed powder of α-Al_2O_3 shown in Fig. 3(b) consists predominantly of small aggregates and primary grains of 0·2 μm diameter.

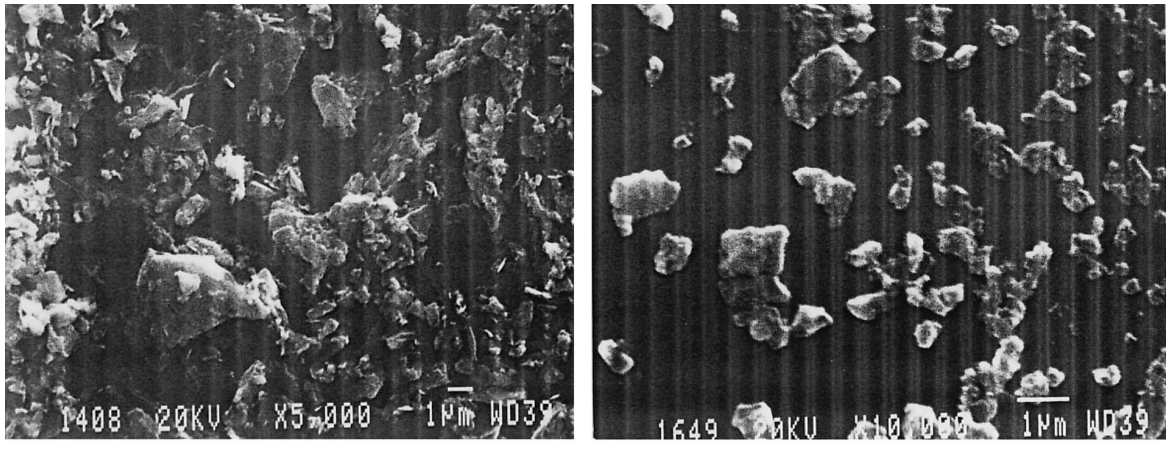

(a) (b)

Fig. 2. SEM photographs of $MgAl_2O_4$ in the original coarse state formed by (a) the preparation process and (b) after grinding according to Table 1.

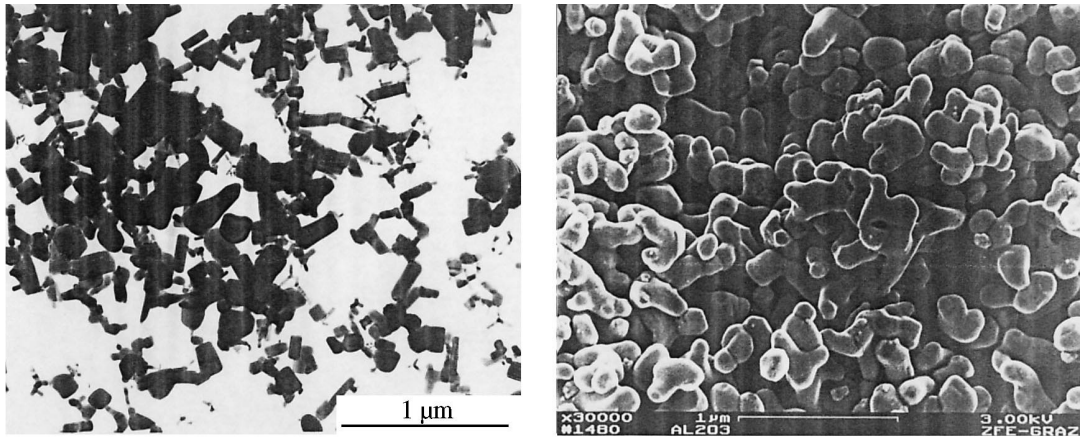

Fig. 3. TEM Photographs of (a) an original ZnO powder and (b) SEM of α-Al_2O_3 .

3 Dielectric Measurements

The dielectric measurements have been carried out using an arrangement of a cylindrical capacitor, whose bottom and displaceable cover act as electrodes:

$$C = \varepsilon_0 \varepsilon_r \frac{A}{L} \qquad \varepsilon_0 = 8{\cdot}859 \times 10^{-12} \frac{As}{Vm} \qquad (1)$$

with A as the area and L as the powder height in the cylinder. According to

$$P = \varepsilon_0(\varepsilon_r - 1)F \qquad (2)$$

with $F = F_0 \exp[i\omega t]$ the permittivity ε_r relates the polarization P to the field strength F. The capacity C of the powders was measured as a function of frequency and volume fraction in air at room temperature and separation of the complex dielectric constant ε^* into real and imaginary part $\varepsilon^* = \varepsilon' - i\varepsilon''$ has been performed. The permittivity values $\varepsilon_r = \varepsilon'$ measured for several volume fractions v_2 in the frequency independent range were found to be suitable for interpretation. However, the conclusion from the permittivity of the mixture of a powder in air to the dielectric constant of the powder itself has to obey the laws of inhomogeneous dielectrics. For a long time inhomogeneous dielectrics have been the matter of extended theoretical studies with the aim to create suitable models for heterogeneous ceramics consisting of several phases or inorganic organic polymer composites or mixtures of powders in air, respectively.

3.1 Measuring equipment

Figure 4 shows a scheme of the measuring apparatus which is similar to those described before by several authors.[2–4] The guard ring at the movable electrode takes care to avoid errors which could rise from field inhomogeneities at the rim. The metallic cylinder containing the powder ensures protection from noise fields. In order to preserve parallel plates the piston with the counter electrode is guided by four metal bars. The volume fraction v_2 was varied in a sufficient range by pressing the powder while varying plate distance L.

The measurements were performed using a HP 4892A LCR meter. Connection type was chosen to be a Four Terminal Pair Configuration[5] to

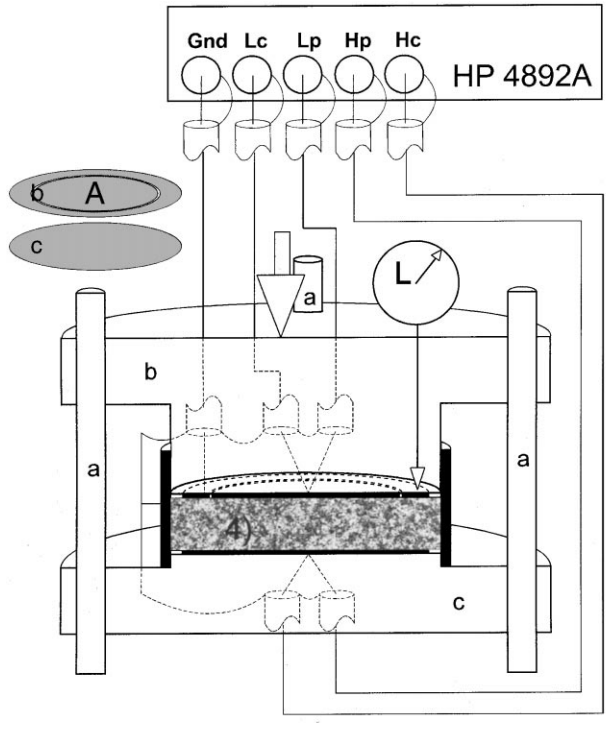

Fig. 4. Setup for measuring the complex permittivity ε^* of mixtures of powders in air. L. dial gauge for distance L; A. electrode area; a. guide bars; b. moving upper electrode; c. fixed bottom electrode; d. sample containment; Gnd...grounded terminal; L_c...low potential side, current path; L_p...low potential side, voltage sensing path; H_c...high potential side, current path; H_p...high potential side, voltage sensing path.

eliminate cable impedances and coupling between current path and voltage sensing cables. Plate distance was measured with a dial gauge with an accuracy of $\pm 0{\cdot}01$ mm.

3.2 Calibration procedure

For checking the reliability of the setup calibration has been carried out measuring liquids of known dielectric constant at different heights L in the cylinder.

According to eqn (1) the permittivity ε_r results from the slope of the linear relationship between C and $1/L$ running through the origin in the absence of stray capacitances. In the measuring range of 1 kHz to about 2 MHz frequency independent ε_r values have been found showing sufficient consistency with the theoretical values. Defining

$$f = \frac{\varepsilon_{r,\text{theor.}}}{\varepsilon_{r,\text{measur.}}} \tag{3}$$

as the correction factor the data of Table 2 indicate straggling around 1. Averaging yields $f = 1{\cdot}00 \pm 0{\cdot}03$ which means that there is no special correction needed and the observed error is $\pm 3\%$.

4 Frequency Dependent Permittivity

Figures 5–7 show the real part $\varepsilon' = \varepsilon_r$ and the imaginary part ε'' of the investigated powders in dependence on frequency at a defined volume fraction v_2. Some of the investigated powders exhibit significant dispersion of the dielectric constant $\varepsilon^* = \varepsilon' - i\varepsilon''$ at lower frequencies. Fortunately, commonly independence of the measuring data of frequency is achieved approaching the range of about 1 to 2 MHz.

In accordance with expectation α-Al_2O_3 shows strictly frequency independent permittivity (Fig. 7). ZnO powders prepared by the French process are known to contain oxygen defects[6] giving rise to a considerable electronic conductivity in the bulk of the small needle-like grains, which could be the reason for the frequency dependent behaviour of ε' and ε'' at lower frequencies. Moreover, in the result of chemisorption of water the surface tends to become covered at least with a mono-layer of OH–ions and additionally in contact with air hydrozincite $Zn_5(OH)_6(CO_3)_2$ may be formed.[7] Despite of drying at 150°C, the rutile powder sample showed a comparatively high frequency dependence of the permittivity (Fig. 7).

It is well known that a heterogeneous mixture composed of two or more phases which differ from each other in dielectric constant and electrical conductivity shows a dielectric dispersion due to the so-called interfacial polarization. Following the Debye approach[8] the polarization rate delayed by a relaxation time has the meaning of a speed to achieve equilibrium. Taking into account that this reaction rate is proportional to the deviation from equilibrium yields the differential equation:

$$\tau \frac{\mathrm{d}P_\omega}{\mathrm{d}t} = P_{\text{stat.}} - P_\omega \tag{4}$$

Separation of a frequency independent part of the polarization according to $P = P_\omega + P_\infty$ leads together with $P_{\text{stat.}} = \varepsilon_0(\varepsilon_{\text{stat.}} - \varepsilon_\infty)\, F$ to the differential equation

$$\tau \frac{\mathrm{d}P_\omega}{\mathrm{d}t} + P_\omega = \varepsilon_0(\varepsilon_{\text{stat.}} - \varepsilon_\infty) F_0 e^{i\omega t}, \tag{5}$$

whose solution is given by

$$P_\omega{}^* = \frac{\varepsilon_{\text{stat.}} - \varepsilon_\infty}{1 + i\omega\tau}\varepsilon_0 F^*$$

with

$$\varepsilon^* = \varepsilon_\infty + \frac{\varepsilon_{\text{stat.}} - \varepsilon_\infty}{1 + i\omega\tau} \tag{6}$$

or after separation in real and imaginary part

$$\varepsilon^* = \varepsilon_\infty + \frac{\varepsilon_{\text{stat.}} - \varepsilon_\infty}{1 + (\omega\tau)^2} - i\frac{(\varepsilon_{\text{stat.}} - \varepsilon_\infty)\omega\tau}{1 + (\omega\tau)^2} = \varepsilon' - i\varepsilon'' \tag{7}$$

According to Debye, when the frequency is increasing the quasi static permittivity $\varepsilon_{\text{stat.}}$ measured at low frequencies drops to a lower constant value

Table 2. Comparison of the measured ε_r-values with liquids of known permittivity

Substance	*Purity*	$\varepsilon_{r,th}(25°C)$	$\varepsilon_{r,meas(1kHz–2MHz)}$	$f_{(1kHz–2MHz)}$
Air	—	1·0006	0·991 ± 0·002	1·010 ± 0,002
Cyclohexane	99%	2·023	1·955 ± 0·003	1·035 ± 0·002
Diethylether	99%	4·34	4·418 ± 0·007	0·982 ± 0·002
Ethylacetate	99·5%	6·02	5·95 ± 0·02	1·011 ± 0·003
1-Pentanole	99%	13·9	14·52 ± 0·07	0·957 ± 0·005

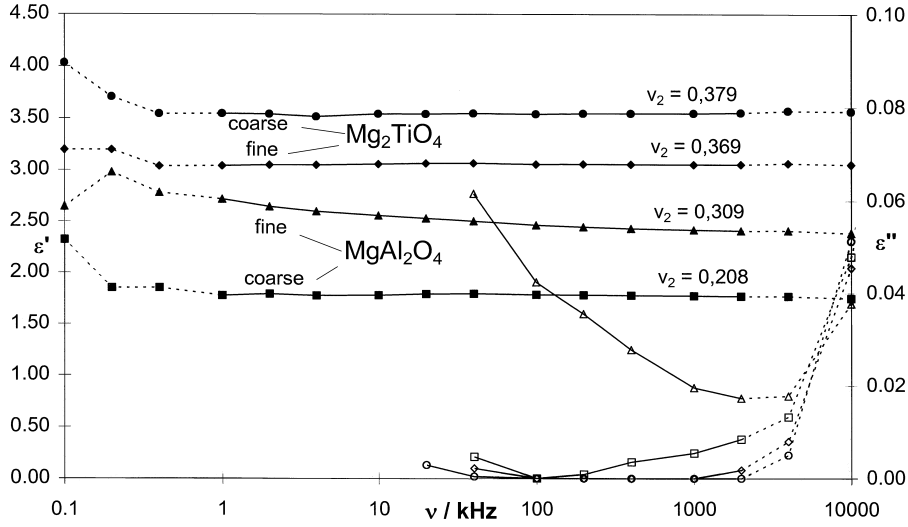

Fig. 5. Frequency dependence of ε' (filled symbols) and ε'' (empty symbols) for the cubic spinel powders Mg_2TiO_4 and $MgAl_2O_4$.

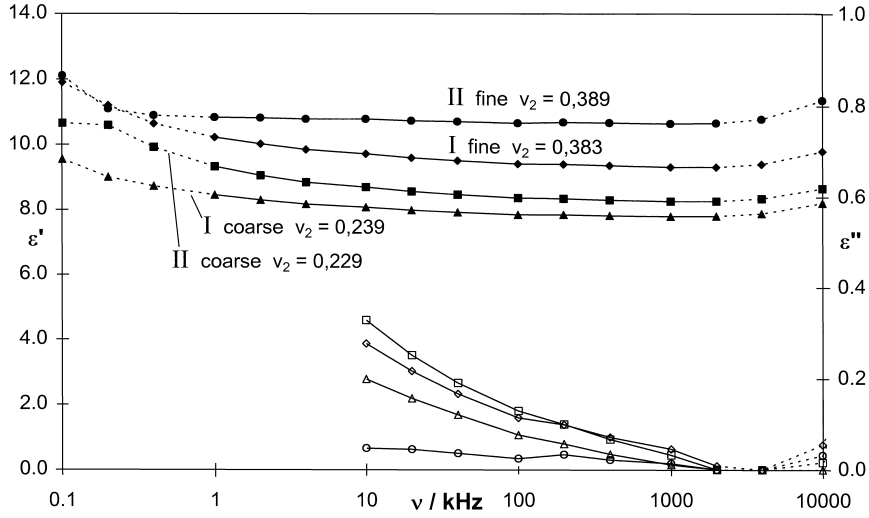

Fig. 6. Frequency dependence of ε' (filled symbols) and ε'' (empty symbols) for $SrTiO_3$ powders with preparation conditions I and II according to Table 1.

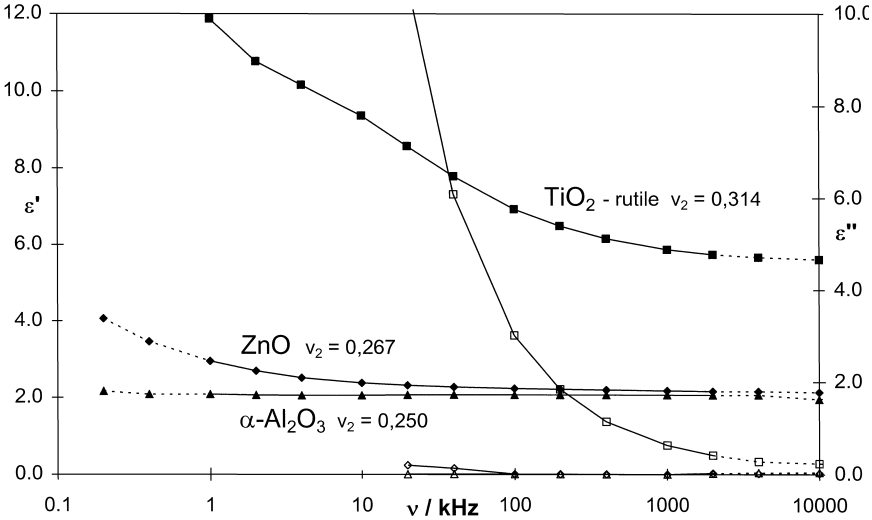

Fig. 7. Frequency dependence of ε' (filled symbols) and ε'' (empty symbols) for the hexagonal powders ZnO and α-Al_2O_3 and tetragonal rutile.

ε_∞, which is predominantly determined by the oscillatory part of the polarization (phonon spectrum) and electron polarization (refraction) of the powder particles. This decrease can often be described by a single relaxation time τ leading to a semiarc in a Cole–Cole-plot.[9] The measured dielectric constants in Figs 5–7 could not be described by a Cole–Cole-semiarc indicating that the observed dielectric dispersion is due to several different mechanisms which may be approached by a distribution function $y(\tau)$ of different relaxation times.[10–12]

$$\varepsilon' = \varepsilon_\infty + \int_0^\infty \frac{y(\tau)d\tau}{1+\omega^2\tau^2} \qquad \varepsilon'' = \int_0^\infty \frac{y(\tau)\omega\tau}{1+\omega^2\tau^2}d\tau \quad (8)$$

However, the resolution of the different mechanisms requires more extended studies which would have exceeded the frame of this paper.

5 The Frequency Independent Real Part of the Permittivity of Powders

Figure 8 shows the data of the dielectric constant $\varepsilon_r = \varepsilon'$ of ZnO and Mg_2TiO_4 powders in dependence on the volume fraction v_2. It can be seen that ε' is increasing with increasing v_2, while the frequency dependence remains approximately unchanged. The other powders have been shown to provide similar results thus leading to the question, by which function the dependence $\varepsilon' = f(v_2)$ can be described. According to Figs 5–8, above about 2 MHz frequency independent values are observed. Hence, this standard frequency was chosen for measuring the $\varepsilon'(v_2)$-curves.

5.1 Theories of inhomogeneous dielectric materials

Studies to deduce the dielectric constant ε' of inhomogeneous materials from the dielectric constants ε_1 and ε_2 of the constituents in dependence on the volume fraction v_2 have been founded in the past already by H. A. Lorentz,[13] L. Lorentz[14] and Raleigh.[15] They derived the relation

$$\frac{\varepsilon' - \varepsilon_1}{\varepsilon' + 2\varepsilon_1} = v_2 \frac{\varepsilon_2 - \varepsilon_1}{\varepsilon_2 + 2\varepsilon_1} \quad (9)$$

for spheres imbedded in a continuous medium with permittivity ε_1 or

$$\frac{\varepsilon' - \varepsilon_1}{\varepsilon' + \varepsilon_1} = v_2 \frac{\varepsilon_2 - \varepsilon_1}{\varepsilon_2 + \varepsilon_1} \quad (10)$$

for cylindrical particles valid for the field direction perpendicular to the axis.

Following Bragg *et al.*[16] and Bernasconi *et al.*[17] an assembly of fairly closely packed ellipsoids of permittivity ε_2 immersed in an infinite medium of dielectric constant $\varepsilon_1 \approx 1$ (air) leads to the following expression for the mean dielectric constant ε':

$$\varepsilon' = 1 + \frac{v_2(\varepsilon_2 - 1)}{1 + D(1 - v_2)(\varepsilon_2 - 1)} \quad \text{Model A} \quad (11)$$

D is the depolarizing coefficient which is a measure of the aspect ratio $\delta = c/a$ of the ellipsoids, that are all oriented parallel to the electric field.

$$D = \frac{1}{\delta^2 - 1}\left[-1 + \frac{\delta}{\sqrt[2]{\delta^2 - 1}} \ln\left(\delta + \sqrt[2]{\delta^2 - 1}\right)\right] \quad (12)$$

With $c = a$ for spheres in accordance with the Lorentz field approximation the value of D is 1/3 thus allowing reduction of eqn (11) to eqn (9).

In real powders of non-spherical particles of unequal shape at random orientation the depolarizing coefficient D is undetermined and locally more or less randomly distributed. Hence, if the

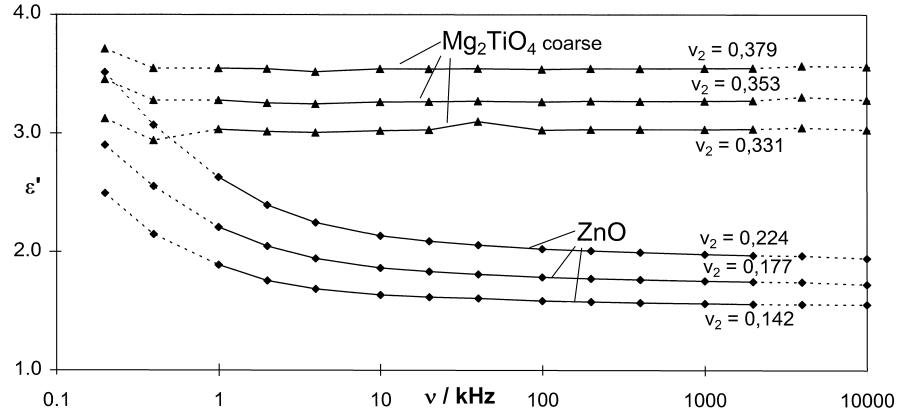

Fig. 8. ε' of Mg_2TiO_4 and ZnO powders in dependence on frequency at different volume fractions v_2.

dielectric constant is known the relationship may be used for estimating a mean value of the depolarizing coefficient D. This value of D has been suggested to be an average measure of the morphology of the powder. Strümpler *et al.*[18] applied the relationship for characterizing dielectric powder polymer composites. They had to assume an aspect ratio of $\delta = 3$ in order to describe the dielectric behaviour of their composites properly.

Bruggeman[19–21] started from an equivalent mixture of two components whose spheres of different size yield at any volume fraction complete space filling. Equation (9) was shown to be transformed into

$$v_2 \frac{\varepsilon_2 - \varepsilon'}{\varepsilon_2 + 2\varepsilon'} + v_1 \frac{\varepsilon_1 - \varepsilon'}{\varepsilon_1 + 2\varepsilon'} = 0 \tag{13}$$

yielding

$$\varepsilon' = \frac{1}{4}\left[2\varepsilon_p - \frac{\varepsilon_s}{\varepsilon_1\varepsilon_2} + 2\sqrt{2(\varepsilon_p - \frac{\varepsilon_s}{\varepsilon_1\varepsilon_2})^2 + 8\varepsilon_1\varepsilon_2}\right] \tag{14}$$

with

$$\varepsilon_p = v_1\varepsilon_1 + v_2\varepsilon_2 \tag{15}$$

according to parallel connection and

$$\varepsilon_s = \frac{1}{\frac{v_1}{\varepsilon_1} + \frac{v_2}{\varepsilon_2}} \tag{16}$$

according to series connection of dielectric spheres of the two materials in a completely filled volume. The equivalent consideration of parallel and series interconnections of particles in an assembly is one of the essential results of the effective medium theory (EMT). A more general derivation has been given by McLachlan[22] with reference to Landauer[23] and Kirkpatrick.[24]

The well known Lichtenecker rule[25]

$$\log \varepsilon = \sum_z v_z \log \varepsilon_z$$

$$\text{or for } z = 2 \tag{17}$$

$$\varepsilon_2 = \exp\left[\frac{1n\varepsilon' - v_1 1n\varepsilon_1}{v_2}\right] \quad \text{Model B}$$

for a two component mixture becomes also plausible from the assumption of equivalent parallel and series interconnections of microcapacitors in a mixture of particles: $\varepsilon^{-1} = \sum_z v_{z,s}\varepsilon^{-1}$ for series and $\varepsilon^{-1} = \sum_z v_{z,p}\varepsilon^1$ for parallel connection $(-1 \le n \le 1)$ leads for equivalent mixing $(v_{z,s} = v_{z,p})$ to $\varepsilon^n = \sum_z v_z\varepsilon^n$ thus yielding for near to zero the relationship $\varepsilon^n = (1+n)\log\varepsilon \approx \log\varepsilon$, i.e. the dielectric particle interaction follows a logarithmic addition rule which is expressed in formula (17) for a mixture of z components with volume fractions v_z.

Recently the Lichtenecker rule has been modified by Wakino.[26] Based on simulation works using the Monte Carlo and the Finite Element Method the following equation has been proposed.

$$\varepsilon_2 = {}^{(v_2 - v_0)}\sqrt{\frac{\exp[(v_2 - v_0)1n\varepsilon'] - v_1\varepsilon_1^{(v_2 - v_0)}}{v_2}} \quad \text{Model C} \tag{18}$$

Computer simulation provides $v_0 = 0{\cdot}35$.

Model B and C neglect the consideration of morphological influences. On the other hand, because of the convenient handling the Lichtenecker model B has been found preferent application.

For polyhedral powder particles Bruggeman[19] proposed a more realistic approach. Starting on the one side from a mixture of spheres randomly embedded in a continuous medium and on the other side from lamellar particles also randomly distributed in a continuous medium he derived the following equations for $\varepsilon'_{\text{sph}}$ and $\varepsilon'_{\text{lam}}$, respectively. Hanai[27] applied Bruggeman's concept using model E for spherical droplets dispersed in an emulsion.

$$1 - v_2 = \frac{\varepsilon_2 - \varepsilon'_{\text{sph}}}{\varepsilon_2 - \varepsilon_1} 3\sqrt{\frac{\varepsilon_1}{\varepsilon'_{\text{sph}}}} \quad \text{for spheres} \quad \text{Model D} \tag{19}$$

$$\varepsilon'_{\text{lam}} = \varepsilon_2 \frac{3\varepsilon_1 + 2v_2(\varepsilon_2 - \varepsilon_1)}{\varepsilon_2 - v_2(\varepsilon_2 - \varepsilon_1)} \quad \text{for lamella} \quad \text{Model E} \tag{20}$$

Following Wiener[28] the formulae (15) and (16) may be interpreted as an upper and lower limit of the dielectric constant ε' for all possible arrangements of particles and aggregates of the constituents. According to

$$\frac{1}{\varepsilon' + u} = \frac{v_1}{\varepsilon_1 + u} + \frac{v_2}{\varepsilon_2 + u}$$

$$\text{and} \tag{21}$$

$$\frac{\varepsilon'}{\varepsilon' + u} = \frac{v_1\varepsilon_1}{\varepsilon_1 + u} + \frac{v_2\varepsilon_2}{\varepsilon_2 + u}$$

$$\text{with } 0 < u < \infty$$

Wiener defined a form number u which leads together with (15) and (16) to

$$\varepsilon' = \frac{\varepsilon_s(\varepsilon_p u + \varepsilon_1\varepsilon_2)}{\varepsilon_1\varepsilon_2 + u\varepsilon_s} \tag{22}$$

The combination of (22) with (19) or (20) allows to express $\varepsilon'_{\text{sph}}$ and $\varepsilon'_{\text{lam}}$ in dependence on the form number u_{sph} or u_{lam}, respectively. For modelling a real powder consisting of polyhedral particles Bruggeman[19] proposed geometric averaging of u_{sph} and u_{lam}. An averaged depolarizing effect of particle shape has been suggested defining $u = \sqrt{u_{\text{lam}} u_{\text{sph}}}$. In this case together with (22) $\varepsilon'(\nu_2)$ only depends on ε_1 and ε_2, i.e. such an approach does not allow shape variation of particles. Indeed, equivalent geometric averaging of the form numbers u_{sph} and u_{lam} implies an artificial limitation. Real powders are expected to contain varying fractions of particles of different shape and size. Therefore we propose to introduce additionally a weighting parameter β in geometric averaging

$$u_{\text{pol}} = 2\sqrt{u_{\text{lam}}^{\beta} u_{\text{sph}}^{2-\beta}} \quad \text{with} \quad 0 \le \beta \le 2 \tag{23}$$

thus leading to

$$\varepsilon'_{\text{pol}} = \frac{\varepsilon_s(\varepsilon_p u_{\text{pol}} + \varepsilon_1\varepsilon_2)}{\varepsilon_1\varepsilon_2 + u\varepsilon_{\text{pol}}\varepsilon_s} \quad \text{Model F} \tag{24}$$

The calculated $\varepsilon'_{\text{pol}}(\nu_2)$ is then determined by ε_1, ε_2. and β. Of coarse, weighting of spherical and lamella-like contributions of particles which are randomly embedded in a continuous medium allows to interpret this parameter β as a form factor reflecting averaged dielectric depolarization caused by particle shape.

Knowing ε_1 of air to be approximately 1·00 the measuring data $\varepsilon'_{\text{pol}}$ are only determined in pairs of ε_2 and β, i.e. it is necessary to introduce ε_2 in order to become aware on the form number β or inverse. Both models A and F show that the higher the dielectric constant of the powder material ε_2 the more the measuring value ε_{pol} is predominantly determined by β. Especially at higher values it seems to be impossible to get information on the dielectric constant ε_2 from powder measurements without knowledge of the depolarization factor D or of the aspect ratio δ (model A) or of the form factor β (model F), respectively.

5.2 Results and discussion

Figure 9 shows a comparison of the $\varepsilon'(\nu_2)$ dependencies of the different models for sample B of coarse $SrTiO_3$ with $\varepsilon_2 = 285$.[29] Neither the Lichtenecker rule (model B) nor the modified version (model C) are able to interpret the measuring data. On the other hand, fitting succeeds sufficiently by combining the boundary models D and E of Bruggeman according to eqns (23) and (24) using the form factor $\beta = 0{\cdot}84$ of model F. In the range of the varied volume fraction the data are also interpretable by model A. However the aspect ratio $\delta = c/a = 6{\cdot}5$ appears artificial in comparison to the measured anisometry. Therefore the polyhedral approach based on combining lamellar and spherical features of particle shape is suggested to be an useful approach in describing the permittivity of powder particles dispersed in air.

Figure 10 shows the results of coarse and ground Mg_2TiO_4 samples. Again, different from the Lichtenecker rule (model B), fitting based on model F with $\varepsilon_2 = 12{\cdot}8$[30] allows powder characterization. Grinding of the coarse powder at the conditions (a), (b) and (c) noticed in Table 1 generates a decrease of the roundness from 10·85 to 2·10, of the bulkiness from 1·19 to 1·03 and of the β value from 0·88 to 0·44 indicating very clearly the increase of spherical contributions to the polyhedral shape of the particles which is in accordance

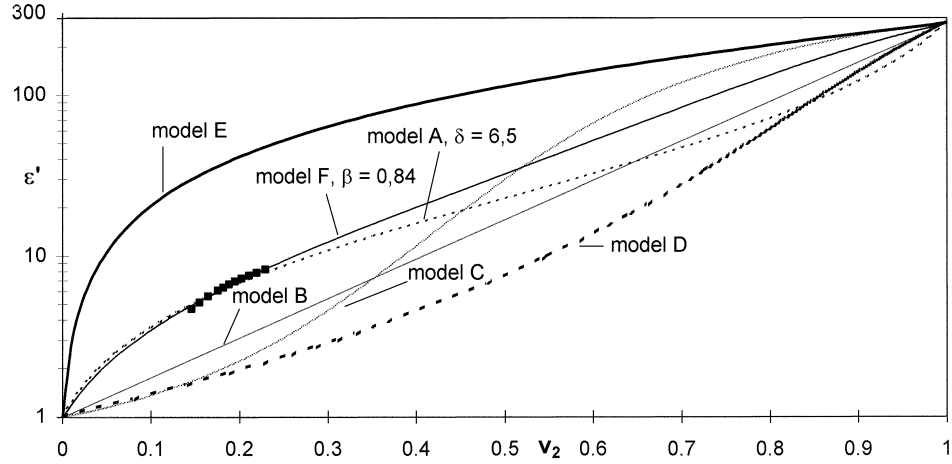

Fig. 9. Measuring data ε' (■) of coarse $SrTiO_3$ (II) in dependence on the volume fraction ν_2 and interpretation based on model F yielding $\beta = 0{\cdot}84$ with $\varepsilon_2 = 285$, or model A with $\delta = 6{\cdot}5$.

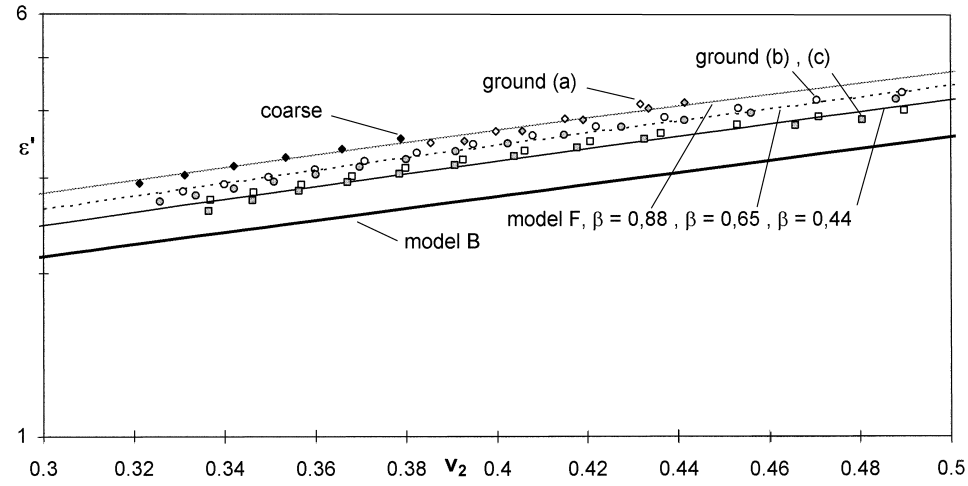

Fig. 10. Permittivity ε' in dependence on the volume fraction v_2 for Mg_2TiO_4 powders in the coarse state and after grinding at the conditions (a), (b), and (c) of Table 1. Together with $\varepsilon_2 = 12{\cdot}8$ the model F fit leads to the β values 0·88 for (a) (◇,◆), 0·65 for (b) (○,●) and 0·44 for (c) (□,■).

with Fig. 1. Double series of measuring points for the powder states (b) and (c) reveal sufficient reproducibility allowing significant interpretation of the different steps of grinding.

Differently from Mg_2TiO_4, the $\varepsilon'(v_2)$ dependencies of the $MgAl_2O_4$ powders in Fig. 11 show an increase of β from 0·60 to 1·0 in the result of grinding, while the anisometry, bulkiness and roundness remain unchanged. Again model B is unsuitable, while model F using for $\varepsilon_2 = 8{\cdot}3$[30] allows successful fitting. Obviously, the flake-like structure of the grains resulting from preparation becomes more effective by grinding, which is indicated by an increase of aspect (lamellar) contributions in the process of dielectric depolarization.

Figure 12 shows the results for $SrTiO_3$ powders (I) and (II) distinguished by different preparation conditions before and after grinding. Again, several independent measuring series show the reproducibility. There is only a small influence of the calcination temperature: (I) 1000°C and (II) 1150°C leading in the coarse state to $\beta = 0{\cdot}84$ or $\beta = 0{\cdot}78$, respectively. On the other hand, grinding causes drastical decrease to $\beta = 0{\cdot}52$ for (I) and $\beta = 0{\cdot}45$ for (II), which indicates the transformation to particles of more spherical contributions. This is also expressed very clearly by the decrease of bulkiness and roundness due to grinding (Table 1). The ground powder state (I) already approximately obeys the Lichtenecker rule. Obviously, far from an approach of complete spherical symmetry (model E) grinding results in polyhedral particle shapes and configurations which involve more and more equivalent contributions of series and parallel interconnections allowing model B to be also a good approximation. Hence, in this case independent of any form number the dielectric constant ε_2 may be deduced from measuring ε' using eqn (17).

As shown in Fig. 13, the coarse powder state of $CaTiO_3$ prepared at 1150°C did not allow to find a fit based on model F. Presumably the high part of comparatively large particles (up to 1 mm) with pronounced microstructure yielding a roundness of 29·63 and a bulkiness of 1·16 were responsible for the extreme course of the measuring points. On the

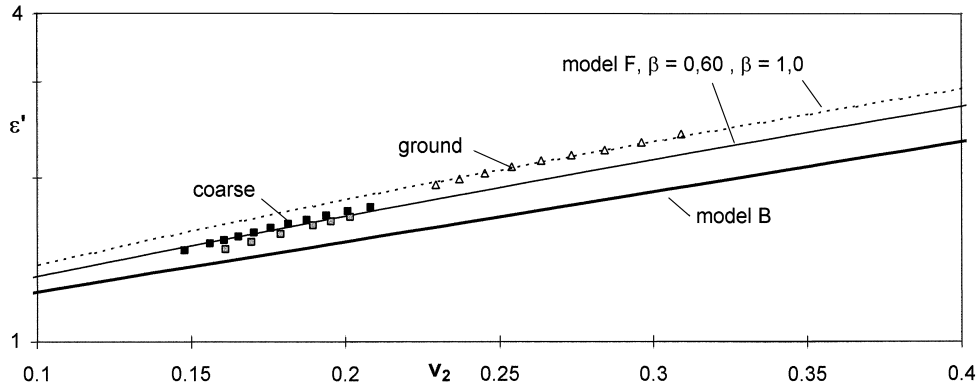

Fig. 11. Permittivity ε' in dependence on the volume fraction v_2 for $MgAl_2O_4$ powders in the coarse state and after grinding, leading to the β values indicated in the figure when $\varepsilon_2 = 8{\cdot}3$ is chosen.

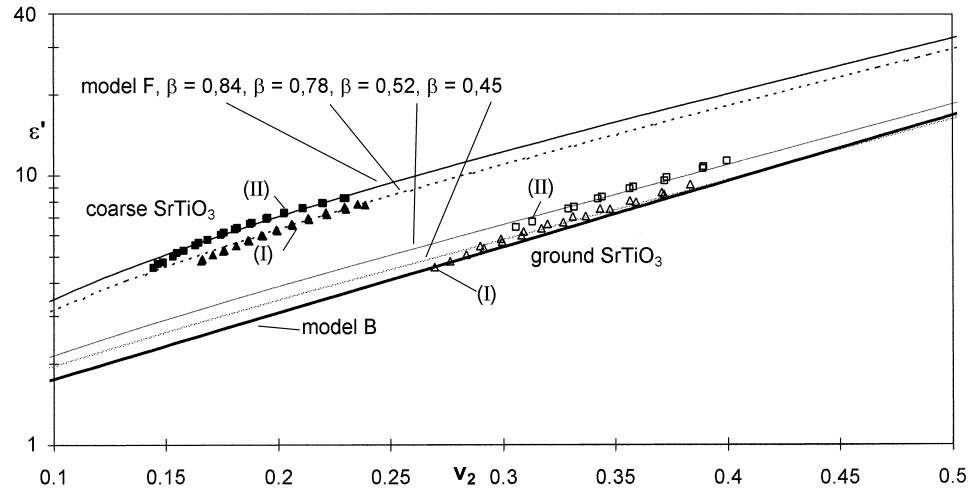

Fig. 12. Permittivity ε' in dependence on the volume fraction v_2 for $SrTiO_3$ (I) (calcined at 1000°C) and $SrTiO_3$ (II) (calcined at 1150°C) before grinding (▲,■) and after grinding (△,□) leading to $\beta = 0{\cdot}84$ for (II) coarse, $\beta = 0{\cdot}52$ for (II) ground, $\beta = 0{\cdot}78$ for (I) coarse and $\beta = 0{\cdot}45$ for (I) ground.

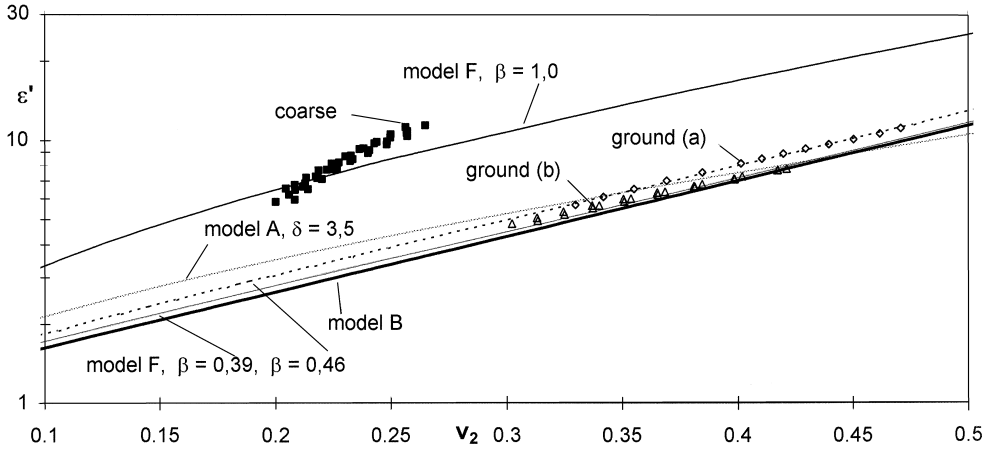

Fig. 13. Permittivity ε' in dependence on the volume fraction v_2 for $CaTiO_3$ before grinding (■) and after grinding according to the conditions (a) (◇) and (b) (△).

other hand, in the result of grinding the values of the shape parameters drop and again fitting based on model F has been performed with $\varepsilon_2 = 130$ for $CaTiO_3$.[29] Model A did not provide sufficient agreement with the measured data. The closest approach providing $\delta = 3{\cdot}5$ is shown in the figure.

Figure 14 shows the fit, that can be obtained with model A or model F for the measured data of α-Al_2O_3 and ZnO powders, while the Lichtenecker rule is not able to interpret the measurements. Based on model A the fit for ZnO using $\varepsilon_2 = 9{\cdot}53$[30] leads to $\delta = 2{\cdot}3$, which is in accordance with the anisometry of 2·39, deduced from the TEM photograph [Fig. 3(a)]. However, it has to be noticed that complete orientation of the particles with their c-axis parallel to the field seems to be unlikely. Again, model F appears as the more realistic approach with the form factor $\beta = 0{\cdot}79$.

For α-Al_2O_3 with $\varepsilon_2 = 10{\cdot}85$[30] model A using $\delta = 2{\cdot}0$ and model F using $\beta = 0{\cdot}54$ yield equally good results which show that model A is obviously also applicable to powders with small ε_2.

Figure 15(a) shows the dependence of the form factor β on anisometry of the investigated powders with exception of the coarse $CaTiO_3$ and the ground $MgAl_2O_4$. These powders have been excluded because of the uncertain form factor β in the first material and of the shape parameters in the latter sample. The increase of β with anisometry indicates very clearly that the new form factor is a true measure of particle shape. At the same time the depolarization factor D calculated from the anisometry is decreasing [Fig. 15(b)]. Moreover, Fig. 15(a) and (b) elucidate a second important factor influencing the form factor β. Regardless to anisometry, coarse and highly aggregated particles showing a high bulkiness and roundness provide extraordinary high β-values. Following the arrow in Fig. 15(a) it can be seen that destruction of Mg_2TiO_4 aggregates by grinding leads to a powder

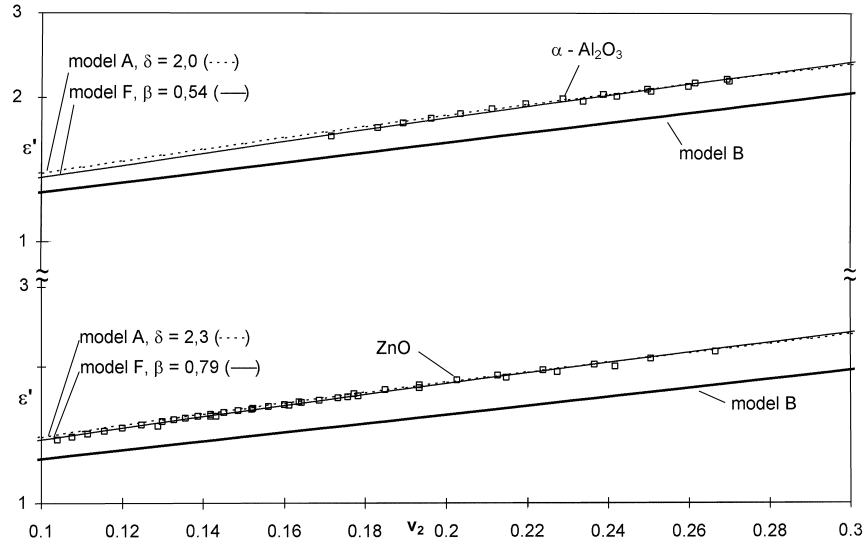

Fig. 14. Permittivity ε' in dependence on the volume fraction v_2 for ZnO ($\varepsilon_2 = 9{\cdot}53$) and α-Al_2O_3 ($\varepsilon_2 = 10{\cdot}85$) and fitting according to model F and model A.

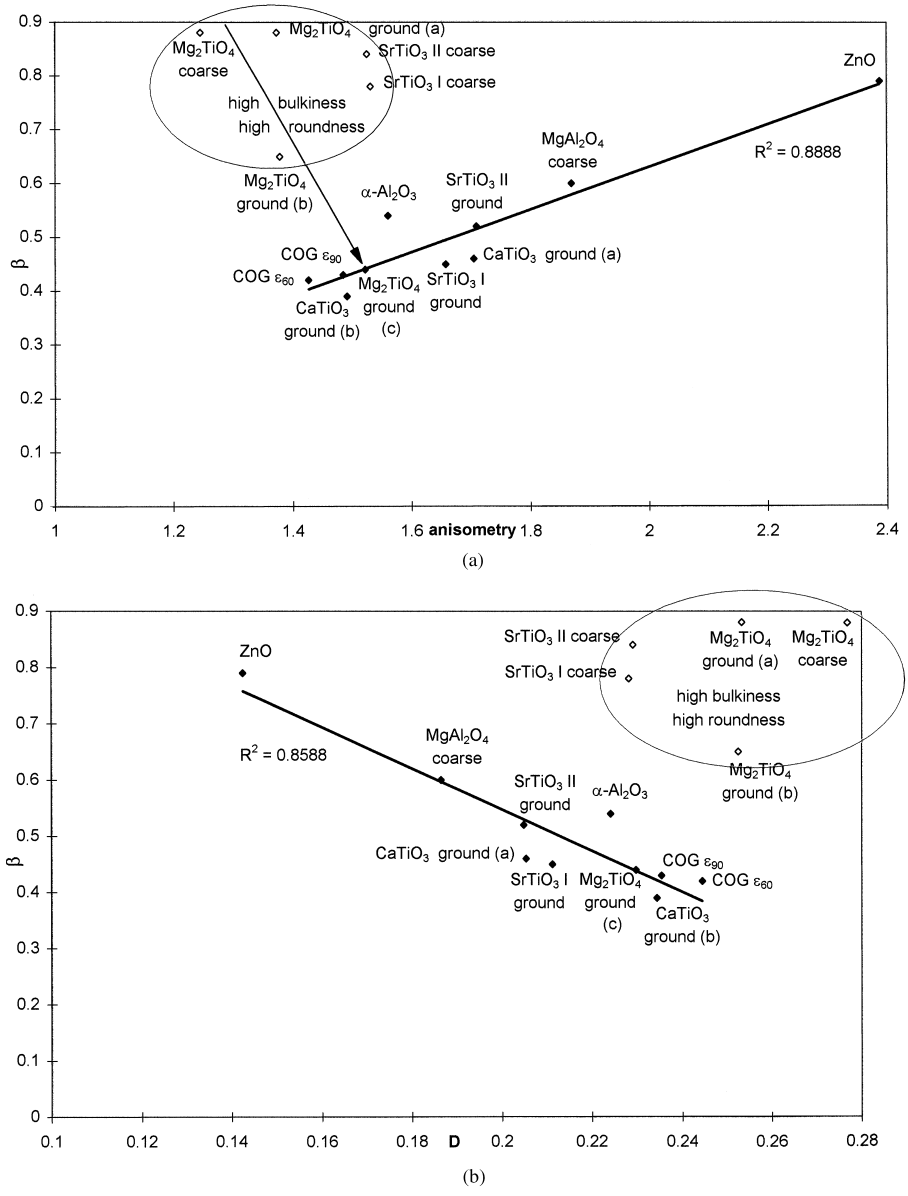

Fig. 15. Correlation of the form factor β to the particle anisometry [Fig. 15(a)] and to the calculated depolarizing coefficient D [Fig. 15(b)]. Only the filled symbols are used to calculate linear regression. Pearson's correlation coefficient R is given.

state that approaches the correlation curve. The dependence of particle bulkiness and roundness on β is also demonstrated in Fig. 16(a) and (b), respectively. β increases with increasing bulkiness and roundness. Again, the high β-value of the ZnO sample indicates the influence of high anisometry on β. Turning again to the Mg_2TiO_4 samples in Fig. 16(b), it is clearly demonstrated that β decreases with the roundness as a result of grinding. Consequently, the measured form factor β is a characteristic of particle shape in two ways: a rugged and porous structure is preferently reflected in high bulkiness and roundness which leads to high β-values. On the other hand, high anisometry gives rise to high β-values.

6 Application to Capacitance Zero Gradient (COG) Capacitor Materials

Figure 17 shows the measuring results of two commercial COG powder materials leading in the ceramic state to the permittivity of $\varepsilon_2 = 60$ or $\varepsilon_2 = 90$, respectively.

X-ray diffraction measurements indicate a multiphase state of the powder. Using these values for the permittivity model F doubtless provides the better approximation than model A. The Lichtenecker rule (model B) is unsuitable for description. The comparison of several lots reveals the degree of achievable resolution in order to detect small differences between lots. The lots of the powder with

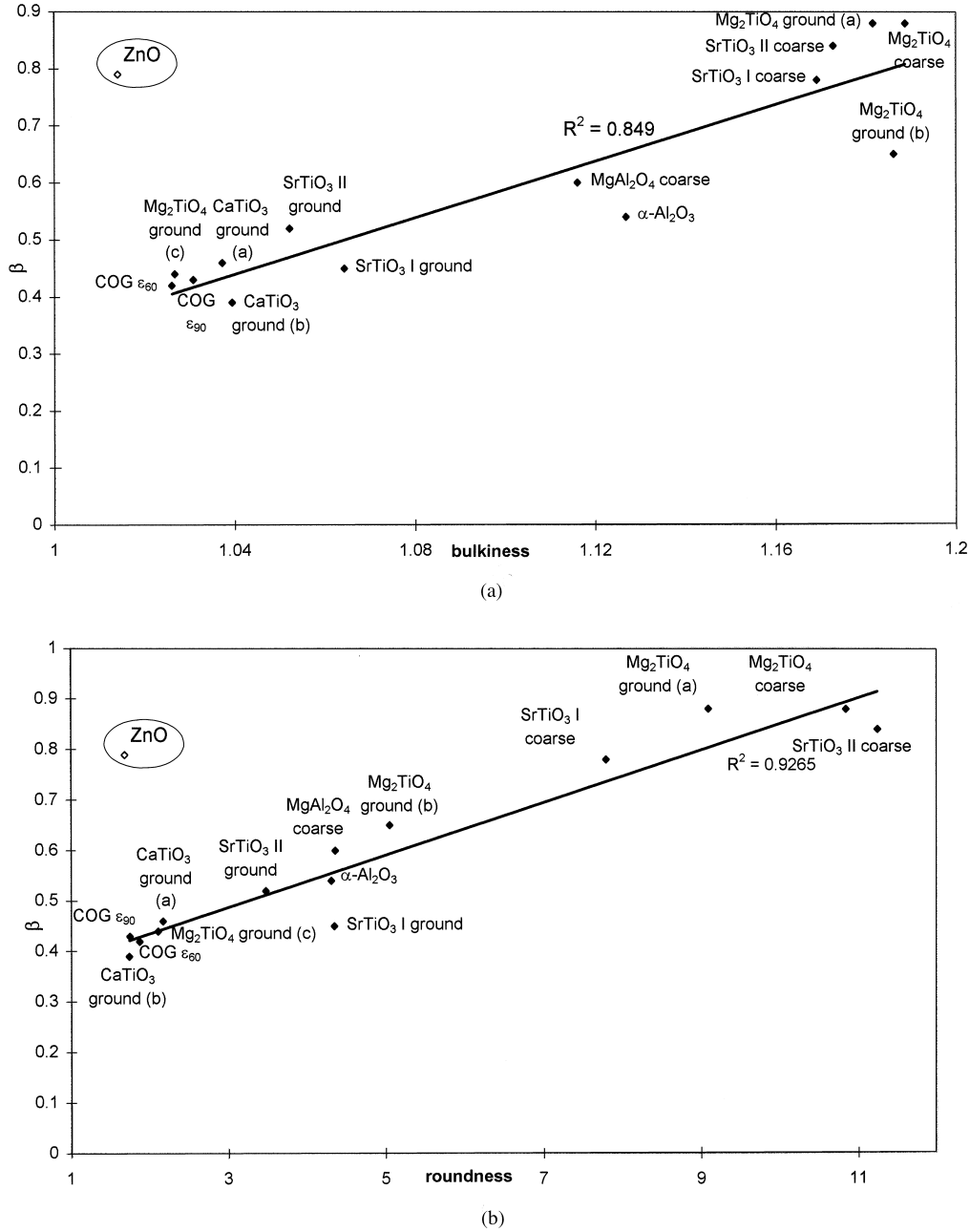

Fig. 16. Correlation of the form factor β to the particle bulkiness [Fig. 16(a)] and to the particle roundness [Fig. 15(b)]. Only the filled symbols are used to calculate linear regression. Pearson's correlation coefficient R is given.

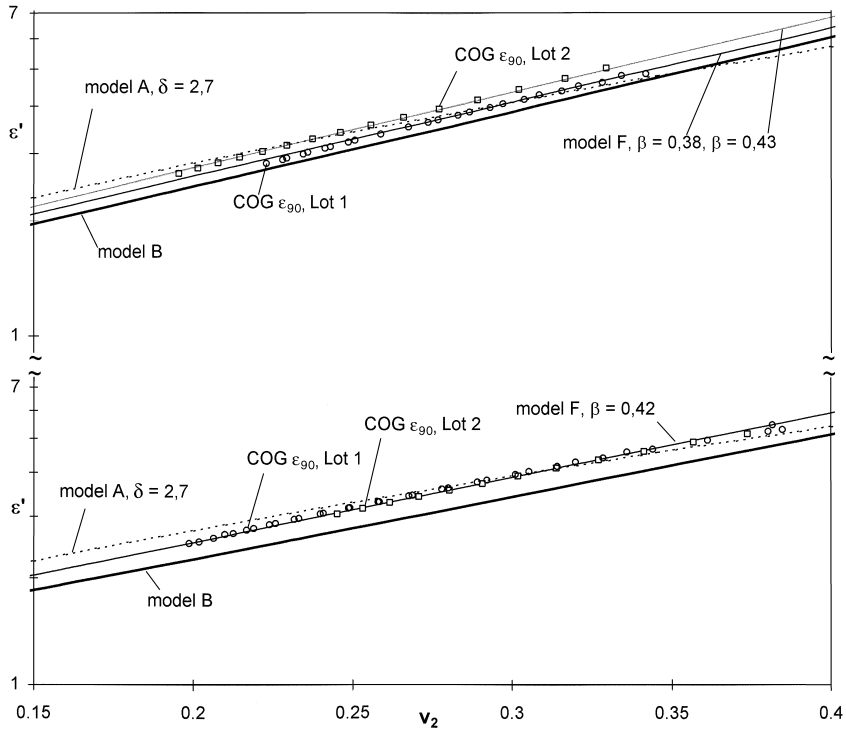

Fig. 17. Permittivity ε' in dependence on the volume fraction v_2 for COG ε_{60} ($\varepsilon_2 = 60$) and COG ε_{90} ($\varepsilon_2 = 90$) capacitor masses.

$\varepsilon_2 = 60$ indicate high reproducibility. Therefore the form number $\beta = 0{\cdot}42$ appears to be representative for this type of a COG raw material. On the other hand, the powder with $\varepsilon_2 = 90$ shows a significant variation of β between 0·38 and 0·43 in a series of six measured lots (only two are drawn in the figure). The specific surface area data of $d_s = 0{\cdot}41\,\mu$m $\pm 0{\cdot}02\,\mu$m and the values of $d_{50} = 0{\cdot}82\,\mu$m $\pm 0{\cdot}04\,\mu$m deduced from grain size distribution measurements reveal a comparable sensitivity of the new defined form number β for characterizing the morphological properties of powders.

7 Summary and Conclusions

Geometrical averaging of Bruggeman's boundary equations using the form factor β allows sufficient interpretation of the frequency independent part of the permittivity of dielectric powders consisting of polyhedral particles embedded in a homogeneous medium, e.g. in air. The permittivity of the solid particles (ε_2) and of the continuous medium (ε_1) have to be known, while the volume fraction (v_2) and the dielectric constant ε' of the mixture are measured.

Qualitatively, β has the physical meaning of a form number giving an information on the morphological state of a powder. The comparison of this model F with the classical approach of model A elucidates a relationship between β and the depolarization factor D, which is a function of the aspect ratio $\delta = c/a$ of morphologically equivalent ellipsoids. However, following the results of this paper model F appears to provide the better approximation. For isometrically shaped powder particles in a highly ground state the Lichtenecker rule seems to lead also to sufficient agreement with the experimental data. The data of the form number β reflect explicitly the anisometry, bulkiness and roundness of the powder particles, BET specific surface area values and grain size distribution measurements. β is found to increase with the anisometry, bulkiness and roundness of the powders. Moreover, the achievable resolution of β indicating small morphological differences is improved with increasing permittivity ε_2 of the powder. The comparability of the β values of powders with different ε_2 showing similar morphological features seems justified. Differences between cubic powder particles on the one side and hexagonal on the other were not resolved by the form number β. The application for checking the reproducibility of multiphase COG powder raw materials allows to detect small morphological differences with a similar resolution as BET specific surface area and grain size distribution measurements.

References

1. Medalia, A. I., Dynamic shape factors of particles. *Powder Tech.*, 1970, **4**, 117–138.
2. Volf, M. and Krenek, F., Measurement of electric quantities of powdered substances. *Sb. Vys. Uceni Tech. Brne*, 1976, **1–4**, 137–146.

3. Kahnt, H., Blayer, A. and Schirrmeister, F., Apparatus for impedance studies of solid ionic conductors. *Exp. Tech. d. Physik*, 1986, **34**, 275–280.
4. Kohlrausch, F., *Praktische Physik*. Vol.2. Teubner, Stuttgart, 1956, pp. 273–323.
5. Honda, M. *The Impedance Measurement Handbook*. Yokogawa-Hewlett-Packard LTD, 1989, 3–1 and 4–11.
6. Teske, K., Oppermann, H. and Stöver, G., Zur Bestimmung der Phasenbreite von Zinkoxid. *Z. anorg. allg. Chem.*, 1984, **511**, 72–76.
7. O'Connor, M. F., A study of the kinetics of the basic Zinc Carbonate formation reaction. *Z. Naturf.,B: Anorg. Chem; Organ. Chem.*, 1974, **29**(3–4)), 202.
8. Daniel, V. V., *Dielectric Relaxation*. Academic Press, London, 1967, pp. 13–31.
9. Cole, K. S. and Cole, R. H., Dispersion and absorption in dielectrics. *J. Chem. Phys.*, 1941, **9**, 341–359.
10. Wagner, K. W., Erklärung der dielektrischen Nachwirkungsvorgänge aufgrund Maxwellscher Vorstellungen. *Arch. Elektrotechn.*, 1914, **2**, 371–387.
11. Yager, W. A., The distribution of relaxation times in typical dielectrics. *Physics*, 1936, **7**, 434–50.
12. Sillars, R. W., The properties of a dielectric containing semiconducting particles of various shapes. *J. Proc. Instn. elect. Engrs.*, 1937, **80**, 378–394.
13. Lorentz, H. A., (1880) *Wied. Ann.*, **9**, 641, refereed after Bruggeman.[17]
14. Lorenz, L., (1880) *Wied. Ann.*, **11**, 70, refereed after Bruggeman.[17]
15. Rayleigh, J. W., (1892) *Phil. Mag.*, **34(5)**, 481, refereed after Bruggeman.[17]
16. Bragg, W. L. and Pippard, A. B., The form birefringence of macromolecules. *Acta Crystallogr.*, 1953, **6**, 865–867.
17. Bernasconi, J., Brüesch, P., Kuse, D. and Zeller, H. R., Ultraviolet to far infrared optical properties of the one-dimensional conductor $K_2Pt(CN)_4Br_{0.3}$. *J. Phys. Chem. Solids*, 1974, **35**, 145–157.
18. Stümpler, R., Rhyner, J. and Greuter, F., Nonlinear dielectric composites. *In Proceedings of SPIE - Int. Soc. Opt. Eng. (USA) Smart structures and materials 1995.*, 2441, **1995**, 256–266.
19. Bruggeman, D. A. G., Berechnung verschiedener physikalischer Konstanten von heterogenen Substanzen I. *Ann. Phys. Lpz.*, 1935, **24**, 636–664.
20. Bruggeman, D. A. G., Berechnung verschiedener physikalischer Konstanten von heterogenen Substanzen I. *Ann. Phys. Lpz.*, 1935, **24**, 665–679.
21. Bruggeman, D. A. G., Berechnung verschiedener physikalischer Konstanten von heterogenen Substanzen II. *Ann. Phys. Lpz.*, 1936, **25**, 645–672.
22. McLachlan, D. S., Equations for the conductivity of macroscopic mixtures. *J. Phys. C: Solid State Phys.*, 1986, **19**, 1339–1354.
23. Landauer, R., The electrical resistance of binary metallic mixtures. *J. Appl. Phys.*, 1952, **23**(7), 779–784.
24. Kirkpatrick, S., Classical transport in disordered media: scaling and effective media theories. *Phys. Rev. Lett.*, 1971, **27**, 1722–1725.
25. Lichtenecker, K., Die Dielektrizitätskonstante natürlicher und künstlicher Mischkörper. *Phys. Ztschr.*, 1926, **27**, 115–158.
26. Wakino, K., Okada, T., Yoshida, N. and Tamono, K., A new equation for predicting the dielectric constant of a mixture. *J. Am. Ceram. Soc.*, 1993, **76**(10), 2588–2594.
27. Hanai, T., Theory of the dielectric dispersion due to interfacial polarization and its applications to emulsions. *Kolloid Z.*, 1960, **171**, 23.
28. Wiener, O. (1912) *Abh. Sächs. Ges. Wiss. Math. Phys. Kl.*, **32**, 509, refereed after Bruggeman.[17]
29. Moulson, A. J. and Herbert J. M., *Electroceramics*. Chapman and Hall, London, 1990, p.234.
30. Shannon, R. D., Dielectric polarizabilities of ions in oxides and fluorides. *J. Appl. Phys.*, 1993, **73**(1), 348–366.